Organic Geochemistry 208 (2025) 105044

Contents lists available at ScienceDirect

Organic Geochemistry

journal homepage: www.elsevier.com/locate/orggeochem

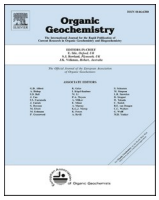

# Sulfur ions reduce the activation energy of steranes and terpanes under hydrothermal action

Rongzhen Qiao, Meijun Li *, Donglin Zhang, Hong Xiao

*Hainan Institute of China University of Petroleum (Beijing), Sanya, Hainan 572025, China*
*National Key Laboratory of Petroleum Resources and Engineering, College of Geosciences, China University of Petroleum (Beijing), Beijing 102249, China*

ARTICLE INFO

Handling Editor: Clifford Walters

*Keywords:*
Hydrothermal alteration
Biomarker
Steranes
Terpanes
Compounds stability
Tarim Basin

ABSTRACT

Steranes and terpanes, as key biomarkers in oils and source rock extracts, provide valuable information about their biological origins, depositional environment, and thermal maturity. The distribution patterns of steranes and terpanes in ultra-deep oil reservoirs within the Shuntuoguole low uplift are complex. The intensity of hydrothermal activity and the influence of sulfur ions were assessed based on the conversion of "Biphenyl–Dibenzothiophene–Phenanthrene" series compounds. The results reveal that the southern sections of F5, F12, and F4 exhibit relatively strong hydrothermal activity (F number: No. number fault zone). The southern sections of F5, F1, and F4 are more significantly impacted by sulfur ion activity under the hydrothermal action. Studies indicate that sterane and terpene concentrations decrease due to sulfur ion activity under the hydrothermal action. Tricyclic terpanes, cholestanes, $C_{31\text{-}35}$ homohopanes, $C_{30}$ hopane, $C_{29}$ diahopane, and pregnane exhibit low stability under the influence of sulfur ion activity in the hydrothermal action. Notably, although tricyclic terpanes, cholestanes, and pregnane show low stability, they are not preferentially depleted. Combined analysis of the relative Gibbs free energies of $C_{30}$ diahopane and $C_{30}$ hopane showed that sulfur ions do not promote pyrolysis by altering the degradation pathways of steranes and terpanes. Instead, sulfur ions likely lower the pyrolysis threshold by reducing the activation energy, preserving the relative stability of steranes and terpanes. This study advances the understanding of organic–inorganic interactions in hydrothermal systems.

## 1. Introduction

Hydrothermal systems typically occur near heat sources in the Earth's crust and are commonly associated with magmatic activity (Large, 1992; Herzig et al., 1998). Hydrothermal processes are a key mechanism for material transfer and exchange from the lithosphere to the outer spheres (biosphere, hydrosphere, and atmosphere) (Sclater et al., 1980; Converse et al., 1984). Hydrothermal fluids are typically composed of water, volatile components (e.g., $H_2S$, HCl, HF, $CO_2$, etc.), and metal ions (e.g., Na, K, Mg, Ca, etc.) (Foustoukos and Seyfried, 2004). It is well established that hydrothermal fluids play a crucial role in the formation of metal deposits, the distribution of gas hydrates, and the transformation of carbonate formations (Davies and Smith, 2006; Hannington et al., 2011; Boetius and Wenzhöfer, 2013). Furthermore, experiments demonstrate that the involvement of water and inorganic compounds typically enhances the reactivity of organic compounds, promoting organic-inorganic interactions (Foustoukos and Seyfried, 2004; Wei et al., 2007; Shipp et al., 2014). For instance, hydrothermal petroleum typically contains substantial amounts of unresolved complex mixture (UCM), higher diamondoids, elevated concentrations of polycyclic aromatic compounds, and distorted molecular geochemistry (Didyk and Simoneit, 1989; Püttmann et al., 1989; McCollom and Seewald, 2006; Xu et al., 2021; Qiao et al., 2024a).

The Paleozoic ultra-deep reservoir in the Tarim Basin contains abundant petroleum resources, with distorted molecular geochemistry (Jia et al., 2010, 2013; Xu et al., 2022; Qiao et al., 2024b). Previous studies have attributed the distorted molecular geochemistry of Paleozoic oils to multiple source rocks. Differential contributions from Lower Ordovician–Cambrian and Middle–Upper Ordovician source rocks have resulted in distinct biomarker profiles and carbon isotopic compositions in these oils (Cai et al., 2009a; Li et al., 2010, 2015; Huang et al., 2016; Zhang et al., 2022). However, sulfur isotope analysis reveals that the majority of Paleozoic oil in the Tarim Basin originates primarily from Cambrian source rocks (Cai et al., 2009b, 2015). Subsequent studies sought to provide a "reasonable" explanation for this discrepancy, focusing on high maturity, secondary alteration, and multi-stage filling

* Corresponding author at: Hainan Institute of China University of Petroleum (Beijing), Sanya, Hainan 572025, China.
*E-mail address:* meijunli@cup.edu.cn (M. Li).

https://doi.org/10.1016/j.orggeochem.2025.105044
Received 11 May 2025; Received in revised form 4 June 2025; Accepted 16 June 2025
Available online 23 June 2025

(Wang et al., 2021; Qiao et al., 2024b; Zhang et al., 2024). Notably, few studies have explored the influence of hydrothermal alteration on the geochemical characteristics of oil. The Tarim Basin has undergone several phases of magmatic activity since the Paleozoic. The Permian Tarim Large Igneous Province (PTLIP) is the largest magmatic activity in the regional geological history, lasting over 37 Ma (Qiao et al., 2025a). This event provided a continuous heat source for the hydrothermal system, and radiometric dating and trace element confirm hydrothermal activity during this period (Li et al., 2024; Qiao et al., 2025b). Additionally, the extensive tangential basement faults and Permian fault reactivation events in the Tarim Basin provided conduits for hydrothermal upwelling (Ning et al., 2022). Numerous traces of silicification, cherts, fluorites, and other hydrothermal alterations observed in the Ordovician reservoirs of the Tarim Basin further confirm the widespread distribution of hydrothermal activity (Dong et al., 2013; Xu et al., 2022).

Xu et al. (2022) examined the "Biphenyl (Bp)–Dibenzothiophene (DBT)–Phenanthrene (Phen)" series compounds conversion during hydrothermal alteration. Subsequently, Qiao et al. (2024a) investigated the distribution of diamondoids under hydrothermal alteration. To date, there have been limited studies on the effects of hydrothermal alteration on steranes and terpanes. To assess the changes in steranes and terpanes under hydrothermal alteration, a series of studies were conducted on 33 Paleozoic oil samples from the Tarim Basin. This study aimed to characterize the distribution patterns of steranes and terpanes under hydrothermal alteration and to evaluate their geochemical stability and interpretive reliability under such conditions.

## 2. Geological setting

The Tarim Basin, the largest oil-bearing basin in western China, covers an area of 5.6 × $10^5$ $km^2$ (Fig. 1a). Surrounded by the West Kunlun, Altyn, and Tianshan mountains, the Tarim Basin consists of four depressions (Kuqa, North, Southwest, and Southeast Depressions) and three uplifts (Tabei, Central, and South Uplifts) (Fig. 1a). Radiometric

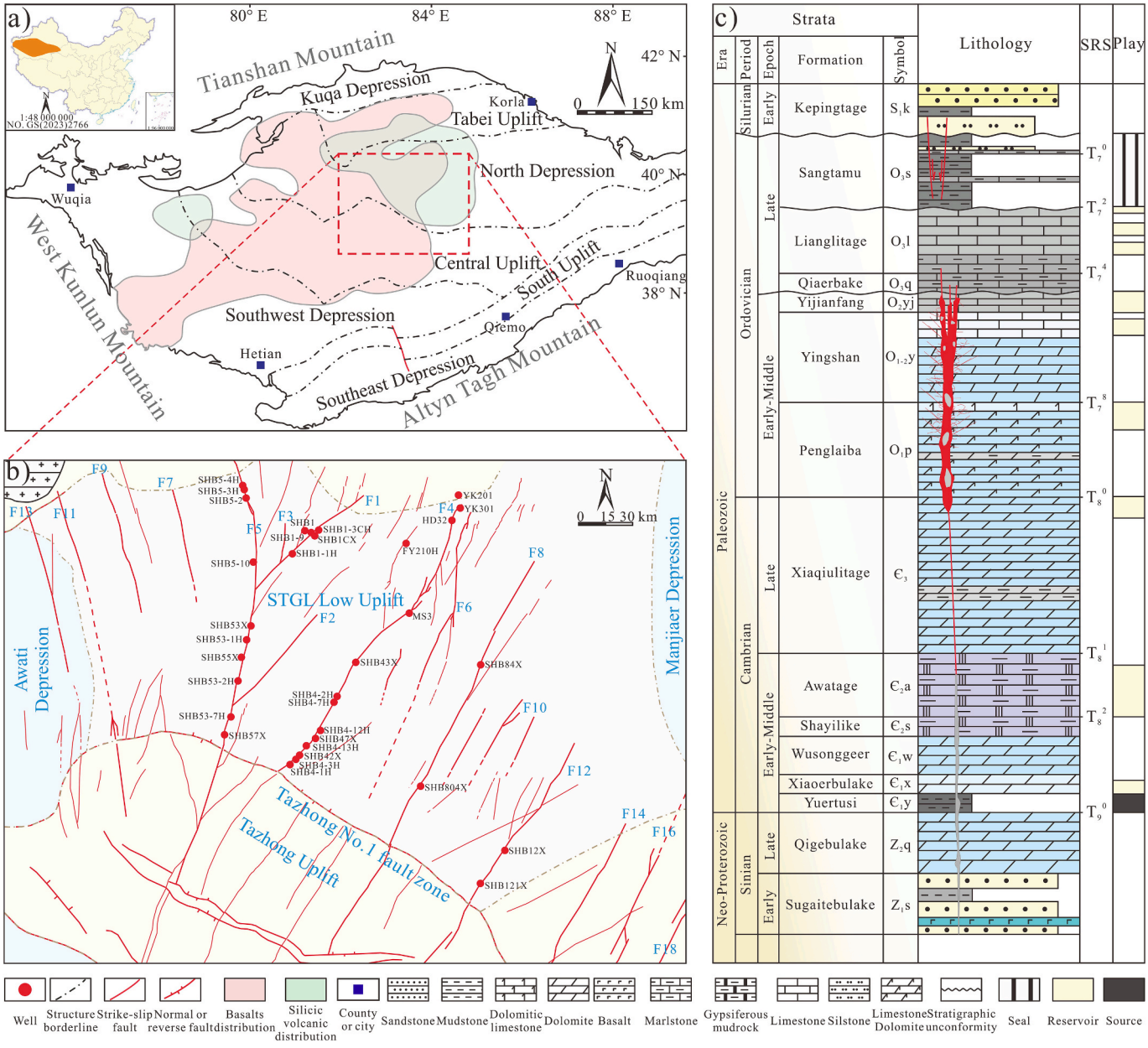


**Fig. 1.** a) Division of tectonic units in the Tarim Basin, with distributions of silicic volcanics and basalts in the PTLIP (refer to Qiao et al., 2025a); b) Geological maps with the fault zone and well location distribution of the STGL low uplift; c) Composite stratigraphic column in the STGL low uplift.

dating of hydrothermal calcite veins indicates multiple phases of hydrothermal activity during the PTLIP (~300–262 Ma) (Qiao et al., 2025a). The PTLIP served as a continuous heat source for hydrothermal activities (Qiao et al., 2025a). Numerous basal-cutting faults in the deep basin serve as key channels for the upward migration of hydrothermal fluids (Ning et al., 2022). The coordination of key elements in the hydrothermal system (fluid, channels, and heat source) triggered large-scale hydrothermal activity during the Permian in the Tarim Basin, leading to the formation of silicification, cherts, fluorites, and other hydrothermal minerals (Dong et al., 2013; Xu et al., 2022).

The study area is the Shuntuoguole (STGL) low uplift, situated in the North Depression (Fig. 1b). Numerous petroleum reservoirs have been identified in the Paleozoic Ordovician, with an average depth exceeding 7000 m (Fig. 1c; Qiao et al., 2024a). The petroleum reservoirs are predominantly located along strike-slip faults, with variations in physical properties and petroleum phase between different fault zones (Qiao et al., 2024b).

## 3. Samples and methods

### 3.1. Samples

This study examines 33 oil samples from Paleozoic Ordovician reservoirs in the STGL low uplift, Tarim Basin. The reservoirs have different types of oil in them, such as light oil, volatile oil, and condensate (Qiao et al., 2024a, 2024b). The detailed classification criteria for petroleum phases are described in Qiao and Chen (2022). Detailed information on sampling and well locations was provided in Supplementary Table S1 and Fig. 1. The oil samples were collected by the author at the wellhead. Given that this study primarily involves volatile samples, including light oil, volatile oil, and condensate, the samples were refrigerated throughout the transport process to China University of Petroleum (Beijing).

### 3.2. Methods

50–60 mg of oil was weighed, and petroleum ether was used for precipitation filtration to remove asphaltenes. The filtrates were subsequently separated into saturated, aromatic, and resin fractions using traditional column chromatography. Organic sulfur compounds were isolated using $Ag^+$ column chromatography following the procedure described in detail by Wei et al. (2012). Briefly, a 10 % $AgNO_3$ solution, prepared with ultrapure water, was added to the activated silica and stirred thoroughly. The mixture was heated at 105 °C for 0.5 h to prepare the silica-supported $Ag^+$, with the entire process conducted under light protection. The asphaltene-free filtrate was introduced to the $Ag^+$ column and sequentially rinsed with petroleum ether, dichloromethane + petroleum ether (2:1, v/v), and dichloromethane + methanol (9:1, v/v). The dichloromethane + methanol (9:1, v/v) mixture elutes the organic sulfur compounds.

Saturated hydrocarbons, aromatic hydrocarbons, whole oils, and organic sulfur compounds were analyzed by GC–MS. The analysis was performed using an Agilent 6890 GC coupled with an Agilent 5975i mass spectrometer, equipped with an HP-PONA quartz capillary column (60 m × 0.25 mm × 0.25 μm). The heating program was as follows: the initial temperature was set to 80 °C and held for 1 min, then increased to 310 °C at a rate of 3 °C/min, followed by a 20 min hold. MS analysis was conducted using electron impact ionization at 70 eV, in full-scan mode with a scan range of 50–600 Da. Quantitative analyses were performed by adding several internal standards, including d50-$C_{24}$ and d16-Adamantane.

## 4. Results

### 4.1. Saturated hydrocarbon compositions

Mass chromatograms (*m/z* 191 and *m/z* 217) revealed obvious differences in the distribution of sterane and terpene biomarkers from the oil samples (Fig. 2). Some oil samples retained the complete series of sterane and terpene biomarkers (Fig. 2a1–c2). However, mass spectrometry (*m/z* 191 and *m/z* 217) of certain oils, such as SHB42X, showed only low levels of $C_{19}$ tricyclic terpene (TT) and $C_{21}$ pregnane (Fig. 2d1 and d2). Quantitative analysis of the sterane and terpene biomarkers in the 33 oil samples revealed concentration ranges of 0.21–410.44 μg/g and 0.19–1620.95 μg/g, respectively (Supplementary Table S1).

### 4.2. Aromatic hydrocarbon compositions

Mass spectrometry (*m/z* 154 + 178 + 184 and *m/z* 168 + 192 + 198) revealed obvious differences in the distribution patterns of Bp, DBT, and Phen compounds in oil samples (Fig. 3). Mass spectrometry (*m/z* 154 + 178 + 184) shows that there are characteristic patterns dominated by Bp, DBT, and Phen compounds, respectively (Fig. 3a1–d1). Furthermore, the distribution patterns of the compounds "Bp–DBT–Phen", "3-methylbiphenyl (MBp)–4-methyldibenzothiophene (MDBT)–(1+3)-methylphenanthrene (MP)", and "4-MBp–(2+3)-MDBT–2-MP" were essentially identical within the same oil sample. That is, they present a "V" shape or an inverted "V" shape, all displaying either a "V"-shaped or inverted "V"-shaped pattern (Fig. 3).

### 4.3. Diamondoids and thiadiamondoids

GC–MS analysis revealed the presence of variable concentrations of diamondoids and thiadiamondoids in ultra-deep oils from the STGL low uplift. Diamondoids and thiadiamondoids, stable cage structures, hold special geological significance. Diamondoids are widely used to assess the maturity (equivalent vitrinite reflectance: Rc; Rc = 0.4389 + 0.0243 * MDI (methyldiamantane index)) and extent of oil cracking (EOC; EOC = 1.2402 * (100 * (1 –$C_o$/$C_c$)) − 28.952, $C_o$: baseline concentration of (3-+4-) methyldiamantane (MD) = 20 μg/g) (Chen et al., 1996; Dahl et al., 1999). Thiadiamondoids are considered effective indicators for TSR identification (Cai et al., 2009a, 2009b, 2022). The maturity and EOC ranges of 33 oil samples were 1.11 %–1.91 % and 0 %–93.20 %, respectively, based on the MDI (MDI = 4-MD/(1-MD + 3-MD + 4-MD)) and the concentration of (3-+ 4-) MD (Supplementary Table S1; Chen et al., 1996; Dahl et al., 1999; Peng et al., 2022). The concentration of thiadiamondoids in oil ranges from 0 to 177.02 μg/g, with significant variability (Supplementary Table S1).

## 5. Discussion

### 5.1. Distorted molecular geochemistry

The distorted molecular geochemistry of Paleozoic Ordovician ultra-deep oils in the Tarim Basin has been extensively studied (Xu et al., 2022; Zhang et al., 2022). The application of sulfur isotope technology has resolved the oil-source debates in the Tarim Basin, establishing Cambrian source rocks as the primary contributors to Paleozoic Ordovician petroleum reservoirs (Cai et al., 2009b, 2015). Previous studies indicate that ultra-deep petroleum in the STGL low uplift is influenced by various secondary processes, yet diamondoids retain their stable characteristics (Qiao et al., 2024a, 2024b). The Rc, derived from the MDI index, effectively evaluates the thermal maturity of oil. The Rc distribution for the 33 oils in this study ranges from 1.11 % to 1.91 %, exhibiting significant variation (Supplementary Table S1). It was previously believed that the decrease in sterane and terpene concentrations resulted from thermal evolution (Zhang et al., 2014; Qiao et al., 2022, 2024c). However, combining reservoir temperature ($T_R$), Rc, sterane

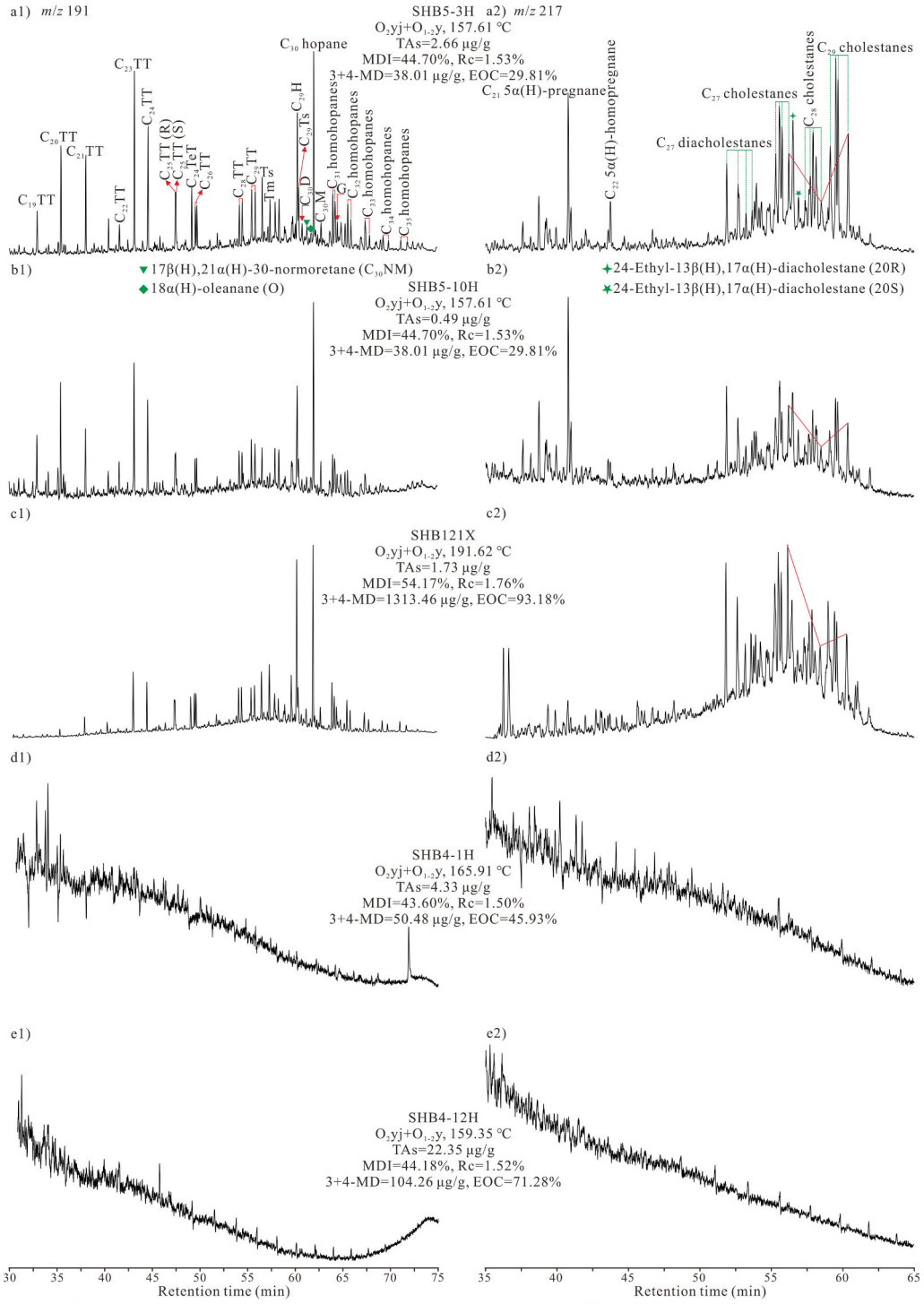


**Fig. 2.** Representative *m/z* 191 (a1–d1) and *m/z* 217 (a2–d2) mass chromatograms in oils from the STGL low uplift.

concentrations, and terpene concentrations reveals that thermal evolution is not the primary cause of the concentration decrease. For example, SHB121X ($T_R = 191.62$ °C; Rc = 1.76 %) exhibits much higher $T_R$ and Rc values, as well as significantly higher concentrations of steranes and terpanes, compared to SHB42X ($T_R = 158.80$ °C; Rc = 1.51 %) (Fig. 2 and Supplementary Table S1). Therefore, the release of steranes and terpanes through kerogen pyrolysis and catalytic hydropyrolysis is unlikely the primary cause of the concentration difference (Seifert, 1978; Mackenzie et al., 1982; Mycke et al., 1987). We need to further investigate the origin of the distorted molecular geochemistry, especially the distribution differences in steranes and terpanes.

### 5.2. Evaluation of hydrothermal activity

Previous studies on hydrothermal activity mainly focused on microscopic observations, isotope analysis, and trace element detection. These studies provide limited identification of hydrothermal activity, lacking quantitative characterization of its intensity or extent. Extensive

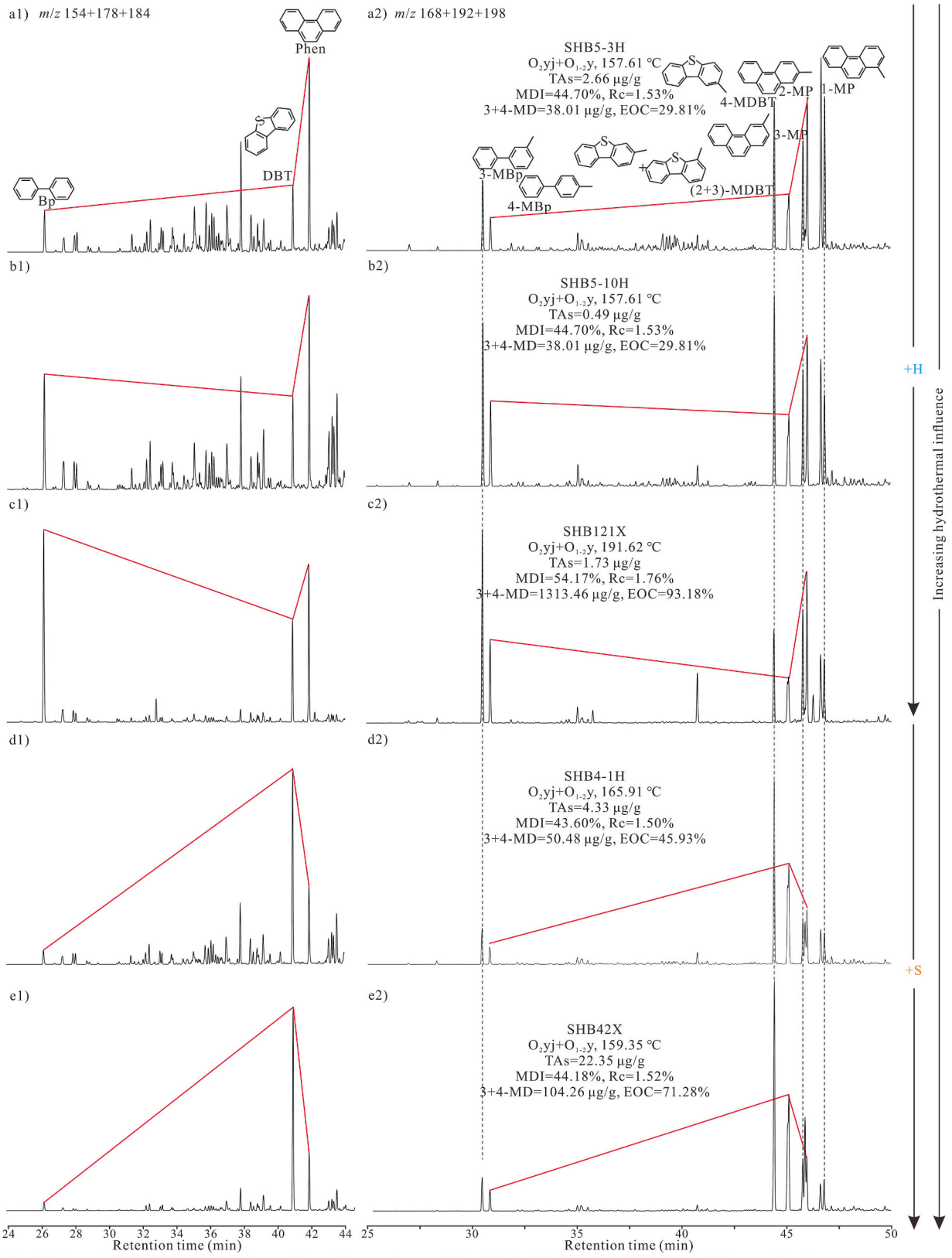


**Fig. 3.** Representative *m/z* (154 + 178 + 184) (a1–d1) and *m/z* (168 + 192 + 198) (a2–d2) mass chromatograms in oils from the STGL low uplift.

evidence of hydrothermal activity has been identified in the Paleozoic Ordovician reservoirs of the STGL low uplift, including silicification, chert, fluorite, and hydrothermal dolomite (Dong et al., 2013; Xu et al., 2022). Previous radiometric dating and trace element research confirmed multiple phases of extensive hydrothermal activity during the PTLIP (Li et al., 2024; Qiao et al., 2025a). The combination of PTLIP (stable heat source) and fault reactivation (channel) led to hydrothermal upwelling and alteration of the petroleum reservoir (Ning et al., 2022; Qiao et al., 2025a). It serves as an ideal natural laboratory for quantitatively assessing the intensity and extent of hydrothermal activity. Xu et al. (2022) demonstrated that hydrothermal activity promotes the interaction of organic-inorganic compounds, such as the mutual conversion of "Bp–DBT–Phen" series compounds by inorganic elements (hydrogen and sulfur ions) (Fig. 4a). However, the influence of TSR on dibenzothiophene series compounds must first be excluded when using the conversion of "Bp–DBT–Phen" series compounds to evaluate hydrothermal activity. Quantitative analysis of thiadiamondoid shows that TSR exists locally in several wells in the southern sections of F4 and F5 (Qiao et al., 2024a, 2025; Wang et al., 2024). The thiadiamondoids concentration in the SHB42X well oil was 41.49 μg/g, indicating a TSR impact (Supplementary Table S1). The sulfur isotope values of dibenzothiophene series compounds range from 19.0 ‰ to 23.2 ‰ (Wang et al., 2024), aligning closely with those in Cambrian source rocks (14.0 ‰–21.6 ‰) (Cai et al., 2009b, 2015) but significantly lower than those in Cambrian gypsum (26.8 ‰–34.1 ‰) (Cai et al., 2016). Previous studies have shown that in the STGL low uplift, only five wells located in the southern section of F4 and F5 are influenced by TSR (Qiao et al., 2024a). This indicates that TSR is limited in reaction degree and has no influence on dibenzothiophene compounds in most samples in this study. Therefore, the "Bp–DBT–Phen" series compounds conversion is a useful method for evaluating ultra-deep hydrothermal activity in the STGL low uplift.

The ternary plots of "3-MBp–4-MDBT–(1+3)-MP" and "4-MBp–(3+2)-MDBT–2-MP" exhibit distinct distribution patterns of oils in the STGL low uplift (Fig. 4 b and c). Sulfur isotope data indicate that Paleozoic Ordovician oils in the STGL low uplift originate from a single source, primarily Cambrian source rocks (Cai et al., 2009b, 2015). Therefore, this variation is likely attributed to hydrothermal activity. In addition to the 33 oil samples analyzed in this study, 55 additional sets of aromatic data were compiled for the contour plots (Supplementary Table S2). Detailed well locations are provided in Supplementary Fig. S1. The relative hydrothermal activity intensity (RHAI) is represented by the ratio of (Bp series + DBT series)/Phen series (Fig. 5). Fig. 5 illustrates that the RHAI in the southern sections of F5, F12, and F4 is significantly higher than in other fault zones of the STGL low uplift. Notably, the oils from the F12 contain a high concentration of steranes and terpanes (Supplementary Table S1).

The "Bp–DBT–Phen" series compounds conversion under hydrothermal activity involves two distinct processes: hydrogen addition (Phen series conversion to Bp series) and sulfur addition (Bp series conversion to DBT series) (Fig. 4a). As the final product of series compound conversion, the DBT series compounds provide convenience for evaluating the influence of sulfur ions under hydrothermal activity. Previous studies have shown that sulfur ion involvement reduces the stability of biomarkers (Cai et al., 2019). The contour plots generated from the 4-MDBT proportion (100 * 4-MDBT/((3 + 1)-MP + 3-MBP + 4-MDBT)) and (2 + 3)-MDBT proportion (100 * (2 + 3)-MDBT/(2-MP + 4-MBP + (2 + 3)-MDBT)) exhibit nearly identical distribution characteristics (Fig. 6a and b). This consistency validates the validity of the "Bp–DBT–Phen" series compound transformation pathway under hydrothermal influence. Furthermore, variations in these ratios can effectively track sulfur ion migration pathways during hydrothermal activity (Fig. 6a and b). The results reveal that the southern sections of F5, F1, and F4 are subject to stronger sulfur ion activity (Fig. 6).

### 5.3. Influencing factors of saturated hydrocarbon biomarkers

Ultra-deep petroleum typically undergoes complex geological processes, where secondary alterations play a significant role (Qiao et al., 2022, 2024c). Previous studies indicate that ultra-deep oil in the STGL low uplift is influenced by the superimposition of various secondary processes, such as biodegradation, oil cracking, TSR, evaporative fractionation, and hydrothermal alteration (Cai et al., 2009a; Qiao et al., 2024a, 2024b; Wang et al., 2024). These alterations likely drive the complex geochemical characteristics and the reduced concentrations of steranes and terpanes in the oil. Through comprehensive analysis of secondary alteration effects, the primary factors responsible for the reduction of sterane and terpane concentrations in oil were identified.

During biodegradation, hydrocarbon-degrading bacteria possess metabolic systems that are related to alkane recognition, transport, and degradation (Rojo, 2009; Perdigão et al., 2021). In addition to *n*-alkanes and *iso*-alkanes, steranes and terpanes are also preferentially degraded (Larter et al., 2003; Peters et al., 2005). However, in the STGL low uplift ultra-deep reservoir, biodegradation is limited to oil entrapped during the Late Caledonian period (Qiao et al., 2024a, 2024b). Furthermore, abundant 25-norhopane compounds were identified in the oil from the STGL low uplift, indicating that the oil had experienced biodegradation above level 6 (Peters et al., 2005). Intact *n*-alkanes were still present, and the oil was predominantly light. This suggests that the biodegraded component, likely formed during the Late Caledonian period, constituted only a minor proportion, indicating that biodegradation had a negligible impact on sterane and terpane distributions. Previous studies

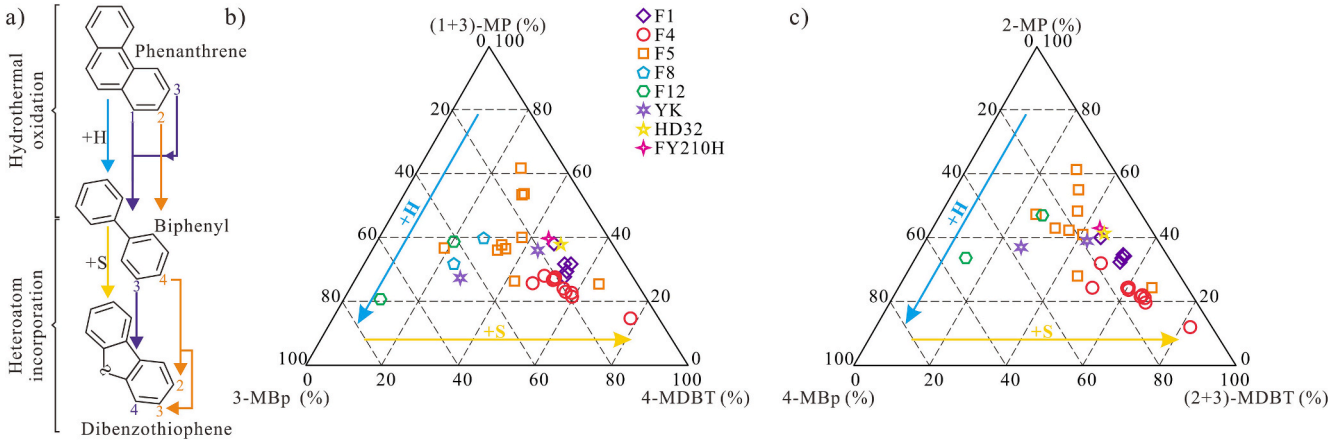


**Fig. 4.** a) Molecular structures and conceptional multiple conversion pathways of PACs (refer to Xu et al., 2022); b) Ternary diagrams showing the relative abundance of b) 3-MBp, 4-MDBT, and (1 + 3)-MP and c) 4-MBp, (2 + 3)-MDBT, and 2-MP.

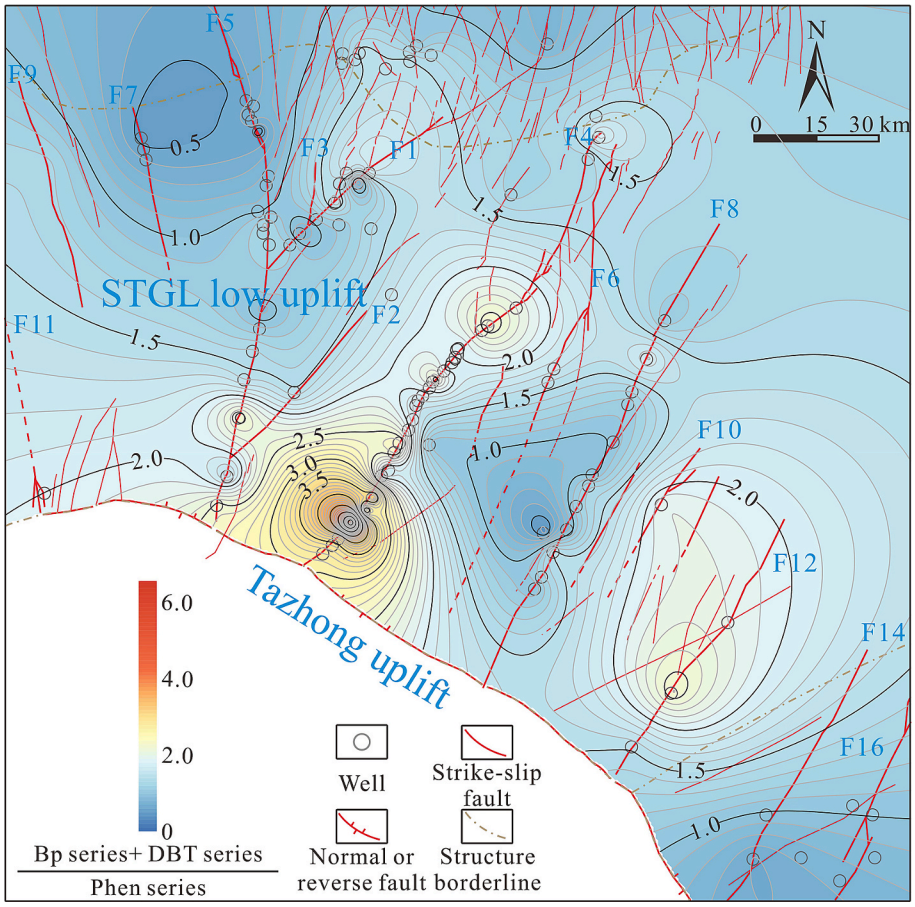


**Fig. 5.** Contour map of the ratio ((Bp series + DBT series)/Phen series) to indicate the relative hydrothermal activity intensity; Bp series = Bp+ (3 + 4)-MBp, DBT series = DBT+ (2 + 3 + 4)-MDBT; Phen series = Phen+(1 + 2 + 3)-MP.

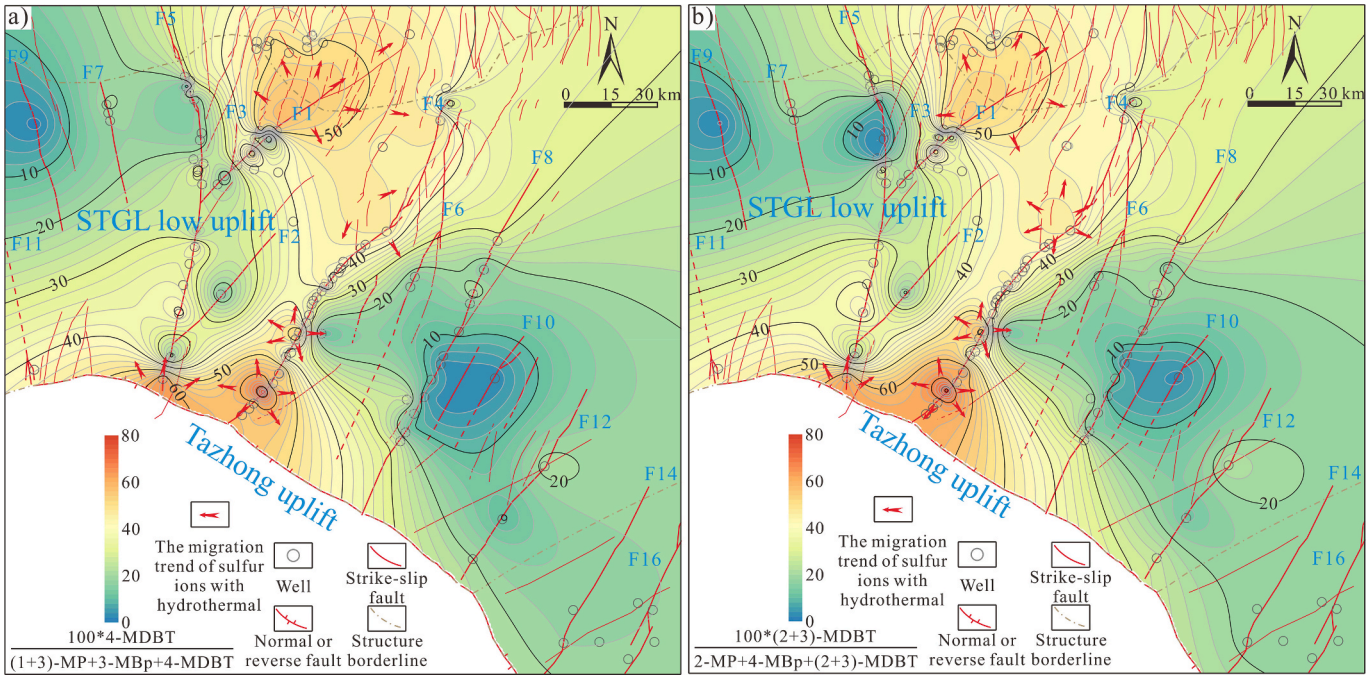


**Fig. 6.** Contour map of the ratios (4-MDBT proportion (a) and (2-+3-) MDBT proportion (b)) to indicate the sulfur ion transport path under hydrothermal activity.

have indicated that evaporative fractionation primarily affects low molecular weight *n*-alkanes and diamondoids, with minimal impact on high molecular weight biomarkers (Qiao et al., 2024c). The toluene/$nC_7$ ratios in the STGL low uplift oils remain consistently low under evaporative fractionation (Qiao et al., 2024a, 2024b). Steranes and terpanes have much higher molecular weights than toluene. Therefore, the effect of evaporative fractionation on steranes and terpanes is also negligible.

Biomarkers controlled by chemical structure exhibit differential distribution during thermal evolution (Peters et al., 2005). Generally, short-chain biomarkers exhibit higher thermal stability than long-chain biomarkers (Lewan, 1997). For homologues, biomarkers with longer side chains are more prone to thermal degradation than those with shorter side chains (Beach et al., 1989). Consequently, the concentrations of steranes and terpanes also decrease during oil cracking. Furthermore, Cai et al. (2019) demonstrated that TSR significantly reduces the concentrations of steranes and terpanes.

Previous studies have shown that diamondoids in oil from the STGL low uplift have not been affected by other secondary effects except for oil cracking (Qiao et al., 2024a). Therefore, the parameters related to diamondoids are reliable. This study selected sterane and terpene concentrations along with 4-MDBT proportion, (2-+3-) MDBT proportion, RHAI, Rc, EOC, and the concentrations of thiadiamondoids (TAs) for the correlation heat map (Fig. 7). The calculation formulas for the relevant parameters are provided in Supplementary Table S1. Sterane and terpene concentrations showed weak correlations with RHAI, Rc, EOC, TAs, reservoir pressure ($P_R$), and Reservoir temperature ($T_R$) (Fig. 7). Previous studies suggested that TSR would also lead to a decrease in the concentrations of steranes and terpanes. In this study, only a few oil samples were affected by TSR. Therefore, we compared the current samples with TSR-affected oils from the Tazhong area. The concentration of TAs in ZG45 oil (TAs = 47.80 μg/g) was similar to that in SHB42X oil (TAs = 41.49 μg/g), and both originated from the Cambrian Yuertusi Formation source rock (Fig. 8; Cai et al., 2015; Qiao et al., 2024b). The terpane compounds in ZG45 oil were almost completely preserved, whereas those in SHB42X oil were nearly completely cracked (Fig. 8a and 8b). This suggests that different controlling factors influenced the terpanes' distribution in the two areas. Additionally, the concentration of TAs in SHB4-1H oil was 4.33 μg/g, below the TSR threshold (20.00 μg/g) defined for the Tarim Basin. This indicates that SHB4-1H oil was not affected by TSR. However, it contained almost no terpane compounds (Fig. 8c). These observations imply that TSR is not the primary factor controlling sterane and terpane depletion in oils from the STGL low uplift. A significant negative correlation was observed with the proportions of 4-MDBT and (2-+3-) MDBT, yielding correlation coefficients ranging from −0.78 to −0.83 (Fig. 7). This suggests that sulfur ions in hydrothermal activity contribute to the reduction of sterane and terpene concentrations. The primary source of sulfur ions is likely thermochemical sulfate reduction (TSR) within the Cambrian reservoirs (Wang et al., 2024; Qiao et al., 2024a). Previous studies have reported that TSR generates abundant intermediate valence sulfur species (e.g., $S^0$ and $S_3^{2-}$) (Wan et al., 2024). These sulfur species migrated upward with hydrothermal fluids into the Ordovician reservoirs, leading to reduced concentrations of steranes and terpanes. Notably, hydrothermal activity can also facilitate TSR (Simoneit and Fetzer, 1996). This may indicate limited hydrothermal fluid transport capacity, which restricted TSR development in most petroleum reservoirs within the STGL low uplift.

### 5.4. *Influence of sulfur ion participation on steranes and terpanes under hydrothermal action*

To further clarify the influence of sulfur ions on steranes and terpanes under hydrothermal action, a comprehensive analysis was carried out based on 4-MDBT proportion and the concentrations of sterane and terpane compounds. Fig. 9 illustrates that the concentrations of steranes and terpanes decrease as a power function of sulfur ion involvement. In addition, concentrations of various steranes and terpanes follow a power function of the 4-MDBT proportion, as shown in the Supplementary Fig. S2. This power function relationship suggests that sulfur ions influence the concentrations of various steranes and terpanes under hydrothermal conditions (Fig. 10a). The results showed that TTs,

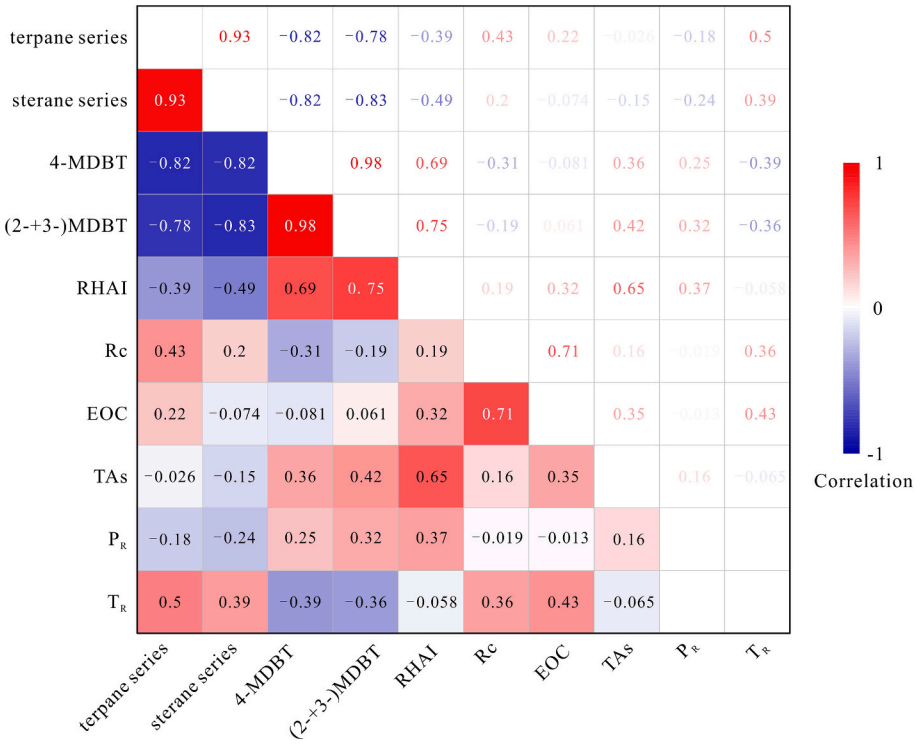


**Fig. 7.** The correlation heat map of steranes and terpanes concentrations with 4-MDBT proportion, (2 + 3)-MDBT proportion, RHAI, Rc, EOC, and TAs concentrations.

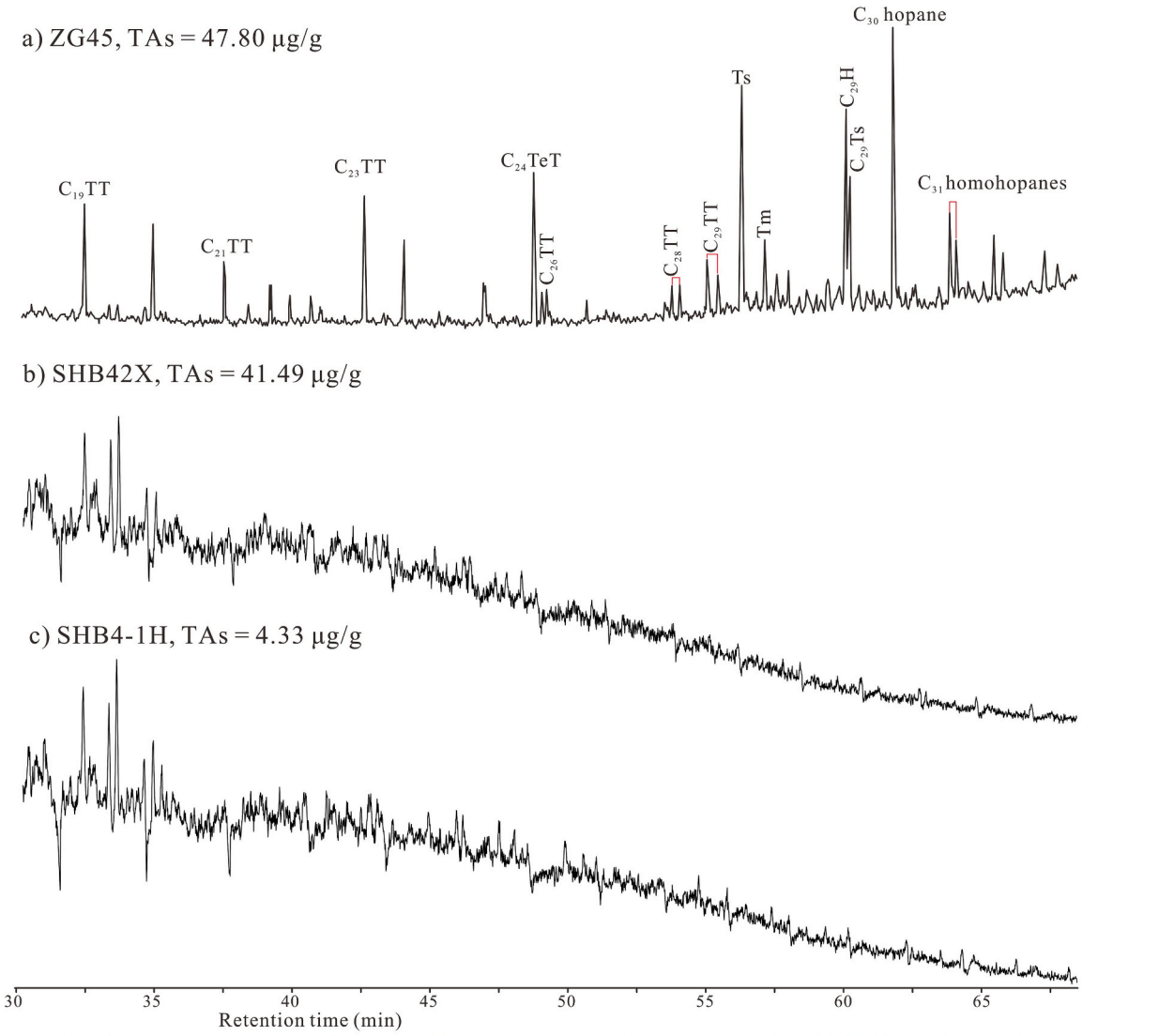


**Fig. 8.** Representative *m/z* 191 mass chromatograms in oils from the Tazhong uplift and the STGL low uplift. a) ZG45 oil, b) SHB42X, and c) SHB4-1H.

cholestanes, $C_{31\text{-}35}$ homohopanes, $C_{30}$ hopane (H), $C_{29}$ diahopane (D), and pregnane have the lowest stability under the influence of sulfur ions in the hydrothermal process (Fig. 10a). It is worth noting that TTs, cholestanes, and pregnane are not preferentially depleted (Figs. 2 and 10a).

Relative Gibbs free energies (ΔG) have been widely applied to assess the thermodynamic stability of isomers (Szczerba and Rospondek, 2010). A previous study based on density functional theory calculations showed that $C_{30}D$ (ΔG = 0 kcal/mol) is thermodynamically more stable than $C_{30}H$ (ΔG = 1.50 kcal/mol) (Xiao et al., 2019). This difference likely arises from variations in molecular structure, particularly the position of the methyl substituents. $C_{30}D$ is relatively stable, as its methyl groups are positioned distally. In contrast, $C_{30}H$ is less stable, primarily due to steric hindrance caused by methyl groups at C-26 and C-27 (Fig. 9b). Under the hydrothermal action, the stability of $C_{30}D$ is still consistently greater than that of $C_{30}H$ with the participation of sulfur ions (Fig. 10b). Therefore, under hydrothermal conditions, sulfur ions may not promote pyrolysis by changing the degradation pathways of steranes and terpanes. Instead, sulfur ions can lower the pyrolysis threshold by reducing the activation energy while maintaining the relative stability of steranes and terpanes. This discovery provides a more reasonable explanation for the variation of the distribution of steranes and terpanes in ultra-deep oil with STGL low uplift.

## 6. Conclusions

In this study, the effects of hydrothermal activity on steranes and terpanes in ultra-deep oil from the STGL low uplift were investigated by means of organic geochemistry. The results show that the conversion of "Biphenyl–Dibenzothiophene–Phenanthrene" series compounds can be effectively applied to evaluate the intensity of hydrothermal activity and the influence of sulfur ions under the hydrothermal action. Among them, the southern sections of F5, F12, and F4 exhibit relatively strong hydrothermal activity. The southern sections of F5, F1, and F4 are more significantly impacted by sulfur ion activity under the hydrothermal action. Studies indicate that sterane and terpene concentrations in the oil decrease due to sulfur ion activity under the hydrothermal action. Tricyclic terpanes (TTs), cholestanes, $C_{31\text{-}35}$ homohopanes, $C_{30}$ hopane (H), $C_{29}$ diahopane (D), and pregnane exhibit low stability under the influence of sulfur ion activity in the hydrothermal action. Notably, although TTs, cholestanes, and pregnane show low stability, they are not preferentially depleted. Combined analysis of the relative Gibbs free

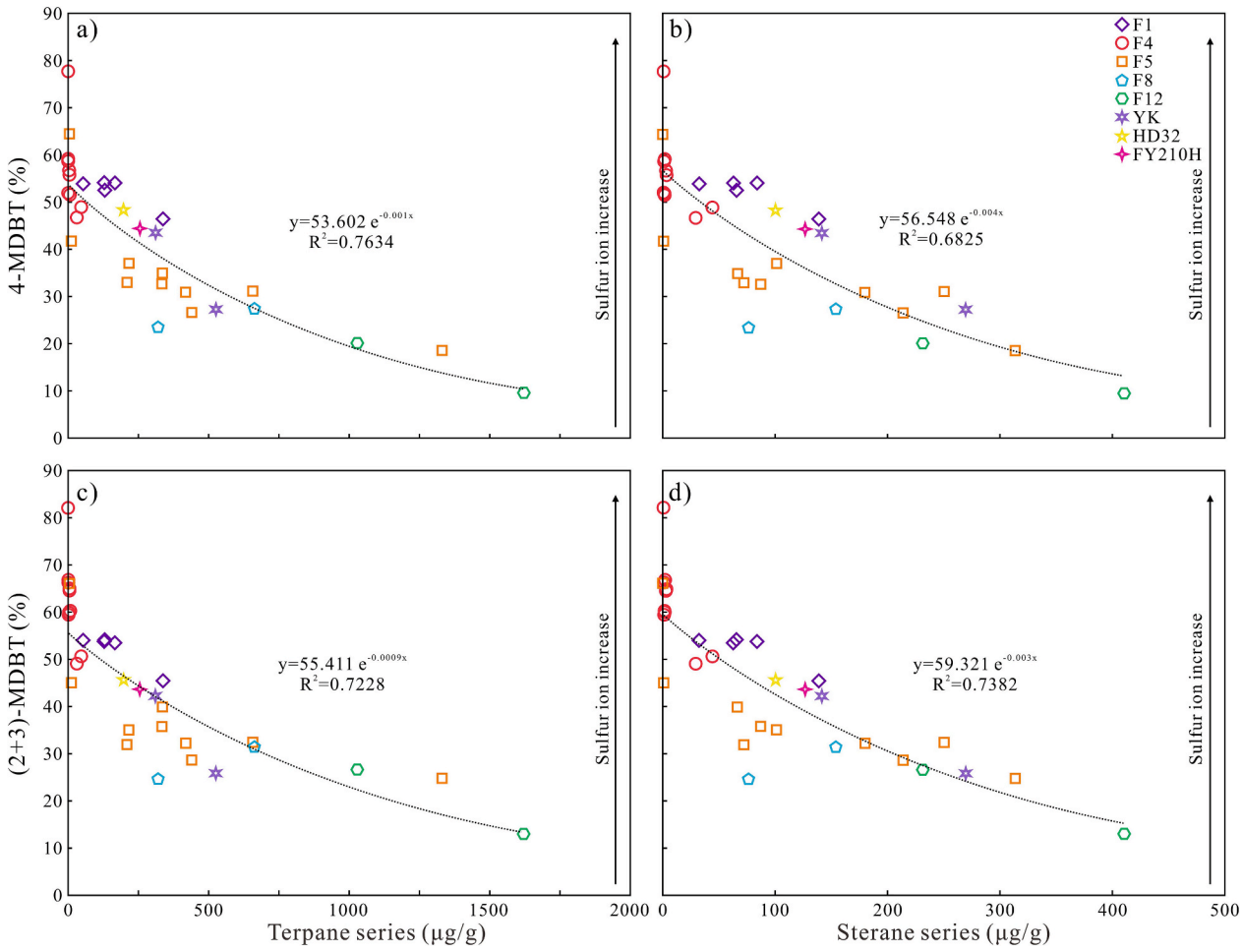


**Fig. 9.** Cross-plots indicating changes in the sterane and terpane concentrations under the involvement of sulfur ions in the hydrothermal action. a) Terpene series concentrations vs. 4-MDBT proportion; b) sterane series concentrations vs. 4-MDBT proportion; c) terpene series concentrations vs. (2 + 3)-MDBT proportion; d) sterane series concentrations vs. (2 + 3)-MDBT proportion.

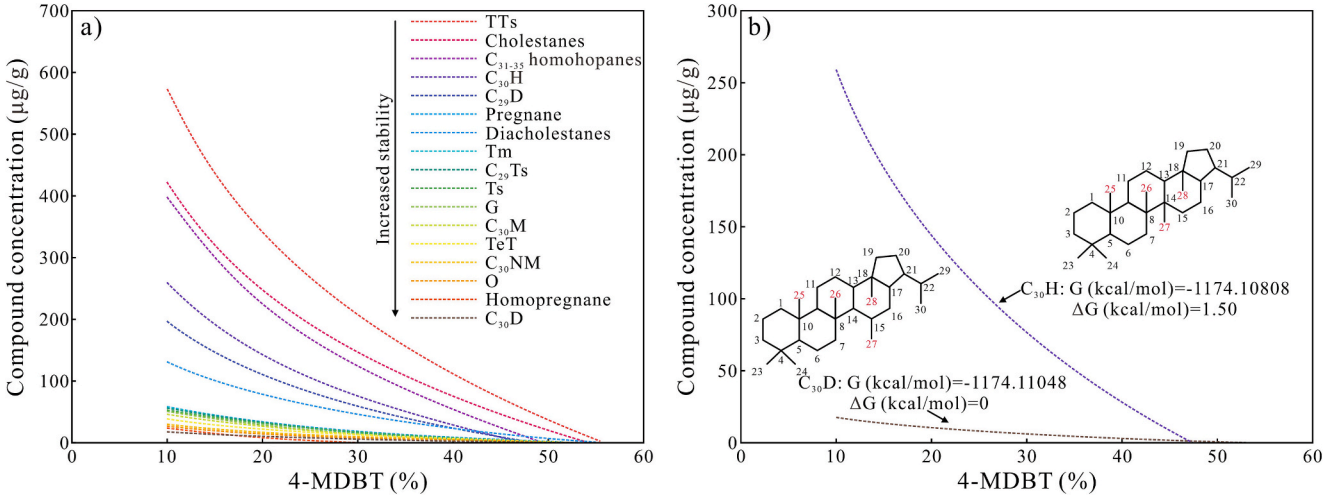


**Fig. 10.** a) Variation of the various sterane and terpane concentrations under the involvement of sulfur ions in the hydrothermal action; b) Variation of the $C_{30}D$ and $C_{30}H$ concentrations under the involvement of sulfur ions in the hydrothermal action, with thermodynamic properties of $C_{30}D$ and $C_{30}H$ at the B3LYP/6-311++G (d, p) level (refer to Xiao et al., 2019).

energies of $C_{30}$D and $C_{30}$H showed that sulfur ions do not promote pyrolysis by altering the degradation pathways of steranes and terpanes. Instead, sulfur ions likely lower the pyrolysis threshold by reducing the activation energy, preserving the relative stability of steranes and terpanes.

## CRediT authorship contribution statement

**Rongzhen Qiao:** Writing – review & editing, Writing – original draft, Validation, Software, Methodology, Investigation. **Meijun Li:** Writing – review & editing, Visualization. **Donglin Zhang:** Software, Methodology, Investigation. **Hong Xiao:** Resources.

## Declaration of competing interest

The authors declare that they have no known competing financial interests or personal relationships that could have appeared to influence the work reported in this paper.

## Acknowledgements

This work was funded by the National Natural Science Foundation of China (Grant No. 42173054).

## Appendix A. Supplementary data

Supplementary data to this article can be found online at https://doi.org/10.1016/j.orggeochem.2025.105044.

## Data availability

Data will be made available on request.

## References

Beach, F., Peakman, T.M., Abbott, G.D., Sleeman, R., Maxwell, J.R., 1989. Laboratory thermal alteration of triaromatic steroid hydrocarbons. Organic Geochemistry 14, 109–111. https://doi.org/10.1016/0146-6380(89)90024-7.

Boetius, A., Wenzhöfer, F., 2013. Seafloor oxygen consumption fuelled by methane from cold seeps. Nature Geoscience 6, 725–734. https://doi.org/10.1038/ngeo1926.

Cai, C.F., Amrani, A., Worden, R.H., Xiao, Q.L., Wang, T.K., Gvirtzman, Z., Li, H.X., Said-Ahmad, W., Jia, L.Q., 2016. Sulfur isotopic compositions of individual organosulfur compounds and their genetic links in the lower Paleozoic petroleum pools of the Tarim Basin, NW China. Geochimica et Cosmochimica Acta 182, 88–108. https://doi.org/10.1016/j.gca.2016.02.036.

Cai, C.F., Li, H.X., Li, K.K., Wang, D.W., 2022. Thermochemical sulfate reduction in sedimentary basins and beyond: a review. Chemical Geology 607, 121018. https://doi.org/10.1016/j.chemgeo.2022.121018.

Cai, C.F., Li, K.K., Ma, A.L., Zhang, C.M., Xu, Z.M., Worden, R.H., Wu, G.H., Zhang, B.S., Chen, L.X., 2009a. Distinguishing the Cambrian source rock from the Upper Ordovician: evidence from sulfur isotopes and biomarkers in the Tarim Basin. Organic Geochemistry 40, 755–768. https://doi.org/10.1016/j.orggeochem.2009.04.008.

Cai, C.F., Tang, Y.J., Li, K.K., Jiang, K.X., Jiang, C.Q., Xiao, Q.L., 2019. Relative reactivity of saturated hydrocarbons during thermochemical sulfate reduction. Fuel 253, 106–113. https://doi.org/10.1016/j.fuel.2019.04.148.

Cai, C.F., Zhang, C.M., Cai, L.L., Wu, G.H., Jiang, L., Xu, Z.M., Li, K.K., Ma, A.L., Chen, L.X., 2009b. Origins of Palaeozoic oils in the Tarim Basin: evidence from sulfur isotopes and biomarkers. Chemical Geology 268, 197–210. https://doi.org/10.1016/j.chemgeo.2009.08.012.

Cai, C.F., Zhang, C.M., Worden, R.H., Wang, T.K., Li, H.X., Jiang, L., Huang, S.Y., Zhang, B.S., 2015. Application of sulfur and carbon isotopes to oil–source rock correlation: a case study from the Tazhong area, Tarim Basin, China. Organic Geochemistry 83–84, 140–152. https://doi.org/10.1016/j.orggeochem.2015.03.012.

Chen, J.H., Fu, J.M., Sheng, G.Y., Liu, D.H., Zhang, J.J., 1996. Diamondoid hydrocarbon ratios: novel maturity indices for highly mature crude oil. Organic Geochemistry 25, 179–190. https://doi.org/10.1016/S0146-6380(96)00125-8.

Converse, D.R., Holland, H.D., Edmond, J.M., 1984. Flow rates in the axial hot springs of the East Pacific Rise (21°N): implications for the heat budget and the formation of massive sulfide deposits. Earth and Planetary Science Letters 69, 159–175. https://doi.org/10.1016/0012-821X(84)90080-3.

Dahl, J.E., Moldowan, J.M., Peters, K.E., Claypool, G.E., Rooney, M.A., Michael, G.E., Mello, M.R., Kohnen, M.L., 1999. Diamondoid hydrocarbons as indicators of natural oil cracking. Nature 399, 54–57. https://doi.org/10.1038/19953.

Davies, G.R., Smith, L.B., 2006. Structurally controlled hydrothermal dolomite reservoir facies: an overview. AAPG Bulletin 90, 1641–1690. https://archives.datapages.com/data/bulletns/2006/11nov/BLTN05164/BLTN05164.HTM.

Didyk, B.M., Simoneit, B.R.T., 1989. Hydrothermal oil of Guaymas Basin and implications for petroleum formation mechanisms. Nature 342, 65–69. https://doi.org/10.1038/342065a0.

Dong, S.F., Chen, D.Z., Qing, H.R., Zhou, X.Q., Wang, D., Guo, Z.H., Jiang, M.S., Qian, Y.X., 2013. Hydrothermal alteration of dolostones in the lower Ordovician, Tarim Basin, NW China: multiple constraints from petrology, isotope geochemistry and fluid inclusion microthermometry. Marine and Petroleum Geology 46, 270–286. https://doi.org/10.1016/j.marpetgeo.2013.06.013.

Foustoukos, D.I., Seyfried, W.E., 2004. Hydrocarbons in hydrothermal vent fluids: the role of chromium-bearing catalysts. Science 304, 1002–1005. https://doi.org/10.1126/science.1096033.

Hannington, M., Jamieson, J., Monecke, T., Petersen, S., Beaulieu, S., 2011. The abundance of seafloor massive sulfide deposits. Geology 39, 1155–1158. https://doi.org/10.1130/G32468.1.

Herzig, P.M., Hannington, M.D., Arribas, A., 1998. Sulfur isotopic composition of hydrothermal precipitates from the Lau back-arc: implications for magmatic contributions to seafloor hydrothermal systems. Mineralium Deposita 1988, 226–237. https://doi.org/10.1007/s001260050143.

Huang, H., Zhang, S., Su, J., 2016. Palaeozoic oil–source correlation in the Tarim Basin, NW China: a review. Organic Geochemistry 94, 32–46. https://doi.org/10.1016/j.orggeochem.2016.01.008.

Jia, W., Xiao, Z., Yu, C., Peng, P., 2010. Molecular and isotopic compositions of bitumens in Silurian tar sands from the Tarim Basin, NW China: characterizing biodegradation and hydrocarbon charging in an old composite basin. Marine and Petroleum Geology 27, 13–25. https://doi.org/10.1016/j.marpetgeo.2009.09.003.

Jia, W., Wang, Q., Peng, P., Xiao, Z., Li, B., 2013. Isotopic compositions and biomarkers in crude oils from the Tarim Basin: oil maturity and oil mixing. Organic Geochemistry 57, 95–106. https://doi.org/10.1016/j.orggeochem.2013.01.002.

Large, R.R., 1992. Australian volcanic-hosted massive sulfide deposits; features, styles, and genetic models. Economic Geology 87, 471–510. https://doi.org/10.2113/gsecongeo.87.3.471.

Larter, S., Wilhelms, A., Head, I., Koopmans, M., Aplin, A., Di Primio, R., Zwach, C., Erdmann, M., Telnaes, N., 2003. The controls on the composition of biodegraded oils in the deep subsurface: Part 1: biodegradation rates in petroleum reservoirs. Organic Geochemistry 34, 601–613. https://doi.org/10.1016/S0146-6380(02)00240-1.

Lewan, M.D., 1997. Experiments on the role of water in petroleum formation. Geochimica et Cosmochimica Acta 61, 3691–3723. https://doi.org/10.1016/S0016-7037(97)00176-2.

Li, S.M., Amrani, A., Pang, X.Q., Yang, H.J., Said-Ahmad, W., Zhang, B.S., Pang, Q.J., 2015. Origin and quantitative source assessment of deep oils in the Tazhong Uplift, Tarim Basin. Organic Geochemistry 78, 1–22. https://doi.org/10.1016/j.orggeochem.2014.10.004.

Li, S.J., Guo, X.W., Wang, B., Cao, Z.C., Xu, H., Chen, J.X., 2024. Recognition of a hydrothermally linked oil accumulation process in the Tahe oil field, northwestern China, with organic geochemistry, Re-Os, and U-Pb geochronology. AAPG Bulletin 108, 1485–1508. https://archives.datapages.com/data/bulletns/2024/08aug/BLTN22124/bltn22124.html.

Li, S.M., Pang, X.Q., Jin, Z.J., Yang, H.J., Xiao, Z.Y., Gu, Q.Y., Zhang, B.S., 2010. Petroleum source in the Tazhong Uplift, Tarim Basin: new insights from geochemical and fluid inclusion data. Organic Geochemistry 41, 531–553. https://doi.org/10.1016/j.orggeochem.2010.02.018.

Mackenzie, A.S., Lamb, N.A., Maxwell, J.R., 1982. Steroid hydrocarbons and the thermal history of sediments. Nature 295, 223–226. https://doi.org/10.1038/295223a0.

McCollom, T.M., Seewald, J.S., 2006. Carbon isotope composition of organic compounds produced by abiotic synthesis under hydrothermal conditions. Earth and Planetary Science Letters 243, 74–84. https://doi.org/10.1016/j.epsl.2006.01.027.

Mycke, B., Narjes, F., Michaelis, W., 1987. Bacteriohopanetetrol from chemical degradation of an oil shale kerogen. Nature 326, 179–181. https://doi.org/10.1038/326179a0.

Ning, F., Yun, J.B., Zhang, Z.P., Li, P., 2022. Deformation patterns and hydrocarbon potential related to intracratonic strike-slip fault systems in the east of Central Uplift Belt in the Tarim Basin. Energy Geoscience 3, 63–72. https://doi.org/10.1016/j.engeos.2021.10.008.

Peng, Y.Y., Cai, C.F., Fang, C.C., Wu, L.L., Liu, J.Z., Sun, P., Liu, D.W., 2022. Diamondoids and thiadiamondoids generated from hydrothermal pyrolysis of crude oil and TSR experiments. Scientific Reports 12, 196. https://doi.org/10.1038/s41598-021-04270-z.

Perdigão, R., Almeida, C.M.R., Magalhães, C., Ramos, S., Carolas, A.L., Ferreira, B.S., Carvalho, M.F., Mucha, A.P., 2021. Bioremediation of petroleum hydrocarbons in seawater: prospects of using lyophilized native hydrocarbon-degrading bacteria. Microorganisms 9, 2285. https://doi.org/10.3390/microorganisms9112285.

Peters, K.E., Walters, C.C., Moldowan, J.M., 2005. The Biomarker Guide, Biomarkers and Isotopes in Petroleum Exploration and Earth History. Cambridge University Press, New York. https://doi.org/10.1017/CBO9780511524868.

Püttmann, W., Merz, C., Speczik, S., 1989. The secondary oxidation of organic material and its influence on Kupferschiefer mineralization of Southwest Poland. Applied Geochemistry 4, 151–161. https://doi.org/10.1016/0883-2927(89)90046-2.

Qiao, R., Chen, Z., 2022. Petroleum phase evolution at high temperature: a combined study of oil cracking experiment and deep oil in Dongying Depression, eastern China. Fuel 326, 124978. https://doi.org/10.1016/j.fuel.2022.124978.

Qiao, R.Z., Chen, Z.H., Li, C.Y., Wang, D.Y., Gao, Y., Zhao, L.Q., Li, Y.Q., Liu, J.Y., 2022. Geochemistry and accumulation of petroleum in deep lacustrine reservoirs: a case

study of Dongying Depression, Bohai Bay Basin. Journal of Petroleum Science and Engineering 213, 110433. https://doi.org/10.1016/j.petrol.2022.110433.
Qiao, R.Z., Li, M.J., Zhang, D.L., Xiao, H., 2024a. Distribution and origin of higher diamondoids in the ultra-deep Paleozoic condensates of the Shunbei oilfield in the Tarim Basin, NW China. Organic Geochemistry 197, 104883. https://doi.org/10.1016/j.orggeochem.2024.104883.
Qiao, R.Z., Li, M.J., Zhang, D.L., Xiao, H., 2024b. Geochemistry and accumulation of the ultra-deep Ordovician oils in the Shunbei oilfield, Tarim Basin: coupling of reservoir secondary processes and filling events. Marine and Petroleum Geology 167, 106959. https://doi.org/10.1016/j.marpetgeo.2024.106959.
Qiao, R.Z., Li, M.J., Zhang, D.L., Chen, Z.H., Xiao, H., 2024c. Evaporative fractionation as the important formation mechanism of light oil reservoirs in the Dongying Depression, NE China. Energies 17, 3734. https://doi.org/10.3390/en17153734.
Qiao, R.Z., Li, M.J., Zhang, D.L., Xiao, H., Wang, W.Q., 2025a. Polycyclic aromatic compounds in crude oil as proxies for Permian Tarim large igneous province activities. Geoscience Frontiers 16, 102000. https://doi.org/10.1016/j.gsf.2024.102000.
Qiao, R.Z., Li, M.J., Zhang, D.L., Xiao, H., 2025b. Enlightenment of geochemistry for ultra-deep petroleum accumulation: coupling of secondary processes and filling events. Petroleum Science 22, 1465–1484. https://doi.org/10.1016/j.petsci.2025.02.019.
Rojo, F., 2009. Degradation of alkanes by bacteria. Environmental Microbiology 11, 2477–2490. https://doi.org/10.1111/j.1462-2920.2009.01948.x.
Sclater, J.G., Jaupart, C., Galson, D., 1980. The heat flow through oceanic and continental crust and the heat loss of the Earth. Reviews of Geophysics 18, 269–311. https://doi.org/10.1029/RG018i001p00269.
Seifert, W.K., 1978. Steranes and terpanes in kerogen pyrolysis for correlation of oils and source rocks. Geochimica et Cosmochimica Acta 42, 473–484. https://doi.org/10.1016/0016-7037(78)90197-7.
Shipp, J.A., Gould, I.R., Shock, E.L., Williams, L.B., Hartnett, H.E., 2014. Sphalerite is a geochemical catalyst for carbon–hydrogen bond activation. Proceedings of the National Academy of Sciences 111, 11642–11645. https://doi.org/10.1073/pnas.1324222111.
Simoneit, B.R.T., Fetzer, J.C., 1996. High molecular weight polycyclic aromatic hydrocarbons in hydrothermal petroleums from the Gulf of California and Northeast Pacific Ocean. Organic Geochemistry 24, 1065–1077. https://doi.org/10.1016/S0146-6380(96)00081-2.
Szczerba, M., Rospondek, M.J., 2010. Controls on distributions of methylphenanthrenes in sedimentary rock extracts: critical evaluation of existing geochemical data from molecular modelling. Organic Geochemistry 41, 1297–1311. https://doi.org/10.1016/j.orggeochem.2010.09.009.
Wan, Q., Wang, X., Hu, W., Wan, Y., Chou, I., 2024. Reaction pathway, mechanism and kinetics of thermochemical sulfate reduction: insights from in situ Raman spectroscopic observations at elevated temperatures and pressures. Geochimica et Cosmochimica Acta 381, 25–42. https://doi.org/10.1016/j.gca.2024.07.027.
Wang, D.W., Kutuzov, I., Zhang, H., Cao, Z.C., Wang, Q.H., Amrani, A., Cai, C.F., 2024. Application of sulfur isotopes of volatile organic sulfur compounds to determine the natural gas secondary alterations and possible sources in the Tarim Basin, NW China. Marine and Petroleum Geology 169, 107078. https://doi.org/10.1016/j.marpetgeo.2024.107078.
Wang, Q., Hao, F., Cao, Z.C., Tian, J.Q., Cong, F.Y., 2021. Geochemistry and origin of the ultra-deep Ordovician oils in the Shunbei field, Tarim Basin, China: implications on alteration and mixing. Marine and Petroleum Geology 123, 104725. https://doi.org/10.1016/j.marpetgeo.2020.104725.
Wei, Z.B., Moldowan, J.M., Zhang, S.C., Hill, R., Jarvie, D.M., Wang, H.T., Song, F.Q., Fago, F., 2007. Diamondoid hydrocarbons as a molecular proxy for thermal maturity and oil cracking: geochemical models from hydrous pyrolysis. Organic Geochemistry 38, 227–249. https://doi.org/10.1016/j.orggeochem.2006.09.011.
Wei, Z.B., Walters, C.C., Moldowan, J.M., Mankiewicz, P.J., Pottorf, R.J., Xiao, Y.T., Maze, W., Nguyen, P.T.H., Madincea, M.E., Phan, N.T., Peters, K.E., 2012. Thiadiamondoids as proxies for the extent of thermochemical sulfate reduction. Organic Geochemistry 44, 53–70. https://doi.org/10.1016/j.orggeochem.2011.11.008.
Xiao, H., Li, M.J., Wang, W.Q., You, B., Liu, X.Q., Yang, Z., Liu, J.G., Chen, Q.Y., Uwiringiyimana, M., 2019. Identification, distribution and geochemical significance of four rearranged hopane series in crude oil. Organic Geochemistry 138, 103929. https://doi.org/10.1016/j.orggeochem.2019.103929.
Xu, H.Y., Liu, Q.Y., Zhu, D.Y., Meng, Q.Q., Jin, Z.J., Fu, Q., George, S.C., 2021. Hydrothermal catalytic conversion and metastable equilibrium of organic compounds in the Jinding Zn/Pb ore deposit. Geochimica et Cosmochimica Acta 307, 133–150. https://doi.org/10.1016/j.gca.2021.05.049.
Xu, H.Y., Liu, Q.Y., Zhu, D.Y., Peng, W.L., Meng, Q.Q., Wang, J.B., Shi, J.Y., Jin, Z.J., 2022. Molecular evidence reveals the presence of hydrothermal effect on ultra-deep-preserved organic compounds. Chemical Geology 608, 121045. https://doi.org/10.1016/j.chemgeo.2022.121045.
Zhang, D.L., Li, M.J., Qiao, R.Z., Xiao, H., 2024. Applicability and limitation of aromatic maturity parameters in high-maturity oil from ultradeep reservoirs. Energy & Fuels 38, 18413–18430. https://doi.org/10.1021/acs.energyfuels.4c02159.
Zhang, S.C., Huang, H.P., Su, J., Zhu, G.Y., Wang, X.M., Larter, S., 2014. Geochemistry of Paleozoic marine oils from the Tarim Basin, NW China. Part 4: Paleobiodegradation and oil charge mixing. Organic Geochemistry 67, 41–57. https://doi.org/10.1016/j.orggeochem.2013.12.008.
Zhang, S.C., Su, J., Wang, X.M., Ma, S.H., 2022. Sedimentary environments of Cambrian–Ordovician source rocks and ultra-deep petroleum accumulation in the Tarim Basin. Acta Geologica Sinica 96, 1259–1276. https://doi.org/10.1111/1755-6724.14982.